Extended Abstracts of the 2008 International Conference on Solid State Devices and Materials, Tsukuba, 2008, pp. 36-37

B-1-5

Source-to-Drain vs. Band-to-Band Tunneling in Ultra-Scaled DG nMOSFETs with Alternative Channel Materials

Quentin Rafhay, Raphaël Clerc, Georges Pananakakis and Gérard Ghibaudo

IMEP-LAHC (INPG-UJF-CNRS)
Minatec, 3 parvis Louis Néel, BP 257, 38016 Grenoble, France- Email: rafhay@enserg.fr

1. Introduction

Thanks to their small effective masses, leading to enhanced quasi ballistic transport properties (higher injection velocity [1] and mean free path [2]) alternative channel materials (such as Ge, GaAs or InGaAs) are expected to outperform on state performances of Si based nano MOSFETs. However, alternative channel material may also increase leakage off state current (fig.1). Several studies have indeed reported an enhancement of Band to Band Tunneling (BBT) leakage mechanism in channel material with small effective masses and small band gap [1,3]. Moreover, in a more recent work considering Source to Drain Tunneling (SDT) (but neglecting BTB), silicon channel has been found to have higher on state performance at same leakage than GaAs and InAs channel devices [4]. In consequence, the theoretical superiority of alternative channel materials in term of I_{on} / I_{off} optimization has not been demonstrated yet, requiring further investigations. And in particular, the relative importance of each leakage mechanism (BBT, SDT and Short Channel Effects -SCEs-) versus materials and device parameters has not been established. The aim of this work is thus to investigate these issues in Double Gate nano nMOSFETs devices. Models and methodology for this comparison are described in section 2, while results are discussed in section 3.

2. Models and methodology

In the on state, devices are supposed to operate in the best condition, i.e. in the full ballistic regime of transport as in [1,3-5], with a single degenerated subband. The Natori approach [6] has been used to model the on state current, accounting for the effect of quantum capacitance degradation [7]. All off state current contributions are then obtained using the same source-drain potential profile, modeled following [8], accounting for the impact of the gate, but also of the source and drain contacts. The transparency of this barrier is then derived using the WKB approach. Both thermionics current (responsible for conventional leakage and enhanced by Short Channel Effects (SCEs)) and SDT contributions (fig.1) are then computed using an Esaki integral over the electron energy [9].

BBT mechanism is known to be difficult to model [10], especially in indirect material, where tunneling is a phonon assisted process. The commonly used models rely on the approaches of Kane [11] for direct bandgap material and of Keldysh [12] for indirect one. These models, due to their great sensitivity on material parameters (fig.2), usually require calibrations using experimental data, which are not always available for alternative channel materials. For this reason, we have compared the Kane and Keldysh models for BTB generation rates to more rigorous Monte Carlo (MC) simulations by Fischetti et al [13]. These analytical models have been found to fairly reproduce MC simulations for all field and materials (fig.3), providing to introduce only one fitting parameter for each model (the exponential prefactor A^d and A^i in Eq. (1) and (2)). Finally, BBT contribution to leakage is calculated by an integration of BBT generation rates over the source-drain subthreshold barrier.

To compare SDT, BBT and SCEs and their impact on device performance versus material parameters, the following procedure has been applied: considering a constant quantization mass equal to $1m_0$, the off and on state currents of DGFETs are calculated for varying transverse transport effective mass m* (fig.4) and varying gap E_g (fig.5). Then, for each device, the metal work function has been adjusted to meet the HP ITRS 2007 off leakage requirements [14].

3. Results and discussions

The on current (I_{on}) of indirect channel material DGFETs designed according to the 16 nm (resp 22nm) node has been plotted in function of m*, for different E_g in Fig. 6 (resp. Fig. 7). It can be seen that a maximum of current is obtained for effective masses around $0.25m_0$ (resp. $0.15m_0$), if E_g is sufficiently large. This maximum results from the competition between two mechanisms enhanced by m* reduction: the beneficial increase of injection velocity [7] in the on state and the detrimental increase of SDT in the off state, explaining results obtained in [4].

At same m* and E_g, BBT generation rates have been found higher in indirect materials than in direct ones (fig.8). This result has been attributed in [12] to the larger density of states available in the conduction band of indirect materials. In consequence, BBT has been found to have a negligible impact on leakage in direct material, whatever are the value of m* and E_g. In indirect materials, the BBT has been found to be the dominant leakage mechanism only when m* and E_g are significantly small (below 1.0 eV and below $0.1m_0$) (fig. 8). In this case, indicated by arrows on fig. 6 and 7, BBT becomes so important that the I_{off} specifications can no longer be satisfied. In all the other cases, SDT has been found to be predominant over BBT and SCEs (fig. 9).

4. Conclusions

In indirect materials with small m* and small E_g material (like Ge [3]), BTB has been found to be the dominant leakage mechanism in nanodevice, preventing to achieve the ITRS leakage requirement. In the other case, SDT dominates leakage, degrading the performance of alternative channel material. Materials with moderate m* (like in the Si case) have been found to offer the best trade-off between I_{on} and I_{off}, explaining results obtained in [4].

5. Acknowledgments

This work has been partially funded by the PULLNANO project (FP6, IST-026828-IP) and the French ANR project Modern.

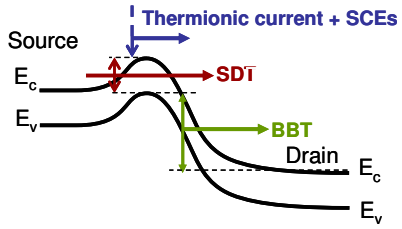

Figure 1 : Scheme of the leakage mechanisms. Thermionic (enhanced by SCEs) electrons pass the barrier with an energy above the top of the barrier; SDT ones tunnel from the source conduction band to the drain one through the barrier; BBT electron tunnel from the valence band to the conduction one on the drain side.

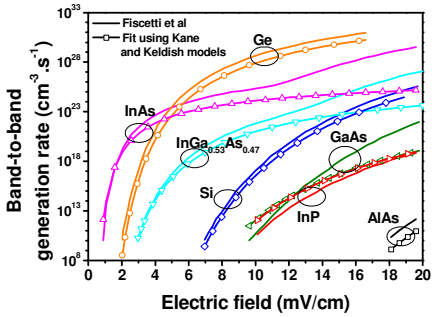

Figure 3 : Band-to-band generation rates vs electric field taken from [13] (straight line) and obtained with the adjusted Kane model [11] for direct materials, and the adjusted Keldysh model [12] for of indirect ones (symbols). A good agreement is obtained considering only two fitting prefactors (one per model – no material dependance).

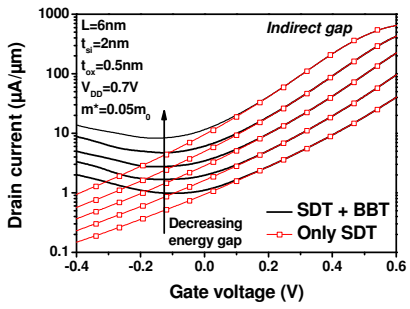

Figure 5 : Subthreshold drain current vs gate voltage including SDT and BBT, or SDT only, for various E_g in indirect materials. Decreasing the energy gap leads to increased minimum current value when BBT is included, while the SDT component is not affected (only V_t shift canceled after Φ_{ms} adjustment).

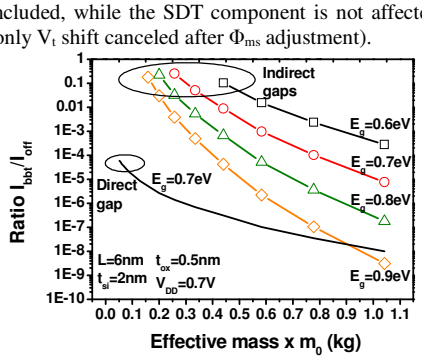

Figure 8: Ratio of the BBT current in direct and indirect material on total I_{off} vs effective mass and different E_g, after Φ_{ms} adjustment. In the case of direct material, the BBT is found negligible whatever are the value of m* or Eg.

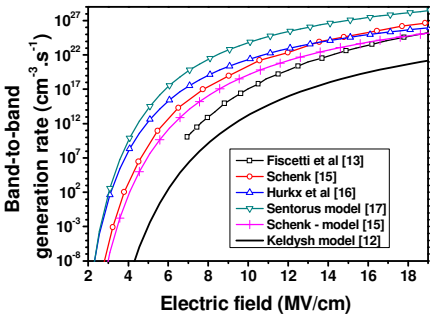

Figure 2 : Band-to-band generation rates in Si vs electric field from various literature references. It can be seen that the without adjustment Keldysh model [12] underestimates the band-to-band generation rate.

Material	Gap (eV)	m_c (m_0)	m_{hh} (m_0)	m_{lh} (m_0)
AlAs	2.14	0.2	0.76	0.15
InP	1.35	0.08	0.6	0.089
GaAs	1.42	0.067	0.51	0.082
Si	1.12	0.191	0.49	0.16
$InGa_{0.53}As_{0.47}$	0.74	0.047	0.45	0.052
InAs	0.36	0.023	0.41	0.026
Ge	0.66	0.08	0.33	0.043

Table 1: Material parameters used this work to obtain the results given in figure 3.

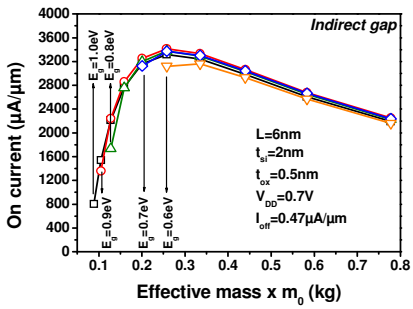

Figure 6: On current vs effective mass for different E_g for the 16nm node of the HP-ITRS 2007 for indirect materials, at constant I_{off}. For a given E_g, The ITRS 2007 I_{off} specification can not be achieved for effective masses below the one indicated by the arrows.

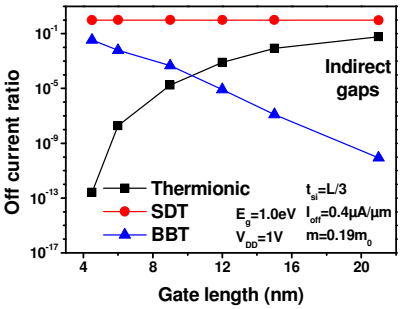

Figure 9 : Ratio of thermionic (+SCEs), SDT and BBT current on the total I_{off} vs gate length. SDT overcomes other leakage mechanisms in the end of the roadmap.

$$R_{bbt}^{dir}(F) = \frac{A^d q^2 \sqrt{m_{//}} F^2}{18\pi\hbar^2 \sqrt{E_g}} \exp\left(-\frac{\pi\sqrt{m_{//}} E_g^{3/2}}{2q\hbar F}\right) \quad (1)$$

$$R_{bbt}^{dir}(F) = \frac{A^i q^{2.5} \sqrt{m_x m_y m_z} F^{2.5} M^2 \upsilon}{2^{5.75}\pi^{2.5}\hbar^{4.5} m_{//}^{1.25} E_g^{1.75}} \exp\left(-\frac{4\sqrt{m_{//}} E_g^{3/2}}{3q\hbar F}\right) \quad (2)$$

$$\text{with} \quad m_{//} = \frac{m_x \cdot m_y}{m_x + m_y}$$

$A^d = 3.10^{-8}$

and $A^i \cdot M^2 \upsilon = 1.10^{65}\ Kg^{-3/2} m^{-9} s^{-1}$

Equations of the band-to-band generation rates for direct (1) and indirect (2) bandgap material, in the Kane [11] and Keldysh [12] models. A^d and A^i are adjusted exponential prefactors.

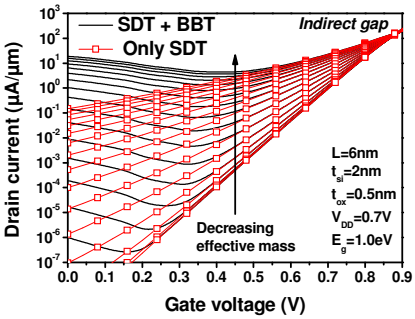

Figure 4 : Subthreshold drain current vs gate voltage including SDT and BBT, or SDT only, for various effective masses in indirect materials. Decreasing effective mass leads to increased subthreshold slope due to SDT and increased minimum current value when BBT is included.

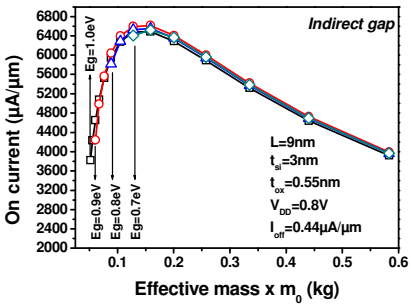

Figure 7: On current vs effective mass for different E_g for the 22nm node of the HP-ITRS 2007 for indirect material, at constant I_{off}. For a given E_g, The ITRS 2007 I_{off} specification can not be achieved for effective masses below the one indicated by the arrows.

References

[1] A. Pethe et al., proc. of IEDM 2005 [2] Q. Rafhay et al., proc. of SSDM 2007 [3] S.E. Laux, IEEE TED vol 54(9) pp.2304-2320 2007 [4] Cantley et al., proc. of IEDM 2007 [5] T. Low et al., proc. of IEDM 2003 [6] K. Natori, JAP 76 (8) 1994 [7] M. De Michielis et al., proc of ESSDERC 2005 [8] Z.-H. Liu, IEEE TED vol 40(1) pp 86-95. 1993 [9] D. K. Ferry, S. M. Goodnick, "Transport in Nanostructure", Cambridge University Press (1997) [10] S. Luryi et al., SSE 51,p212-218, 2007 [11] E.O. Kane, J. Appl. Phys. Vol 32(1) pp 83-91 1961 [12] L.V. Keldysh, Sov. Phys JEPT, vol 6, no 4, pp763-770, 1958 [13] M.V. Fischetti et al., IEEE TED vol 54(9) pp.2116-2136, 2007 [14] ITRS 2007 http://www.itrs.net/ [15] Schenk, SSE, vol 36(1) pp. 19-34 1993 [16] G.A.M. Hurkx et al., IEEE TED, vol 39(2) pp. 331-338 1992 [17] Sentorus user guide, pp249